International Journal of Mechanical, Industrial and Aerospace Sciences
ISSN: 2517-9950
Vol:3, No:10, 2009

A Hybrid Overset Algorithm for Aerodynamic Problems with Moving Objects

S. M. H. Karimian, F. S. Salehi, and H. Alisadeghi

***Abstract*—**A two-dimensional moving mesh algorithm is developed to simulate the general motion of two rotating bodies with relative translational motion. The grid includes a background grid and two sets of grids around the moving bodies. With this grid arrangement rotational and translational motions of two bodies are handled separately, with no complications. Inter-grid boundaries are determined based on their distances from two bodies. In this method, the overset concept is applied to hybrid grid, and flow variables are interpolated using a simple stencil. To evaluate this moving mesh algorithm unsteady Euler flow is solved for different cases using dual-time method of Jameson. Numerical results show excellent agreement with experimental data and other numerical results. To demonstrate the capability of present algorithm for accurate solution of flow fields around moving bodies, some benchmark problems have been defined in this paper.

***Keywords*—** Moving mesh, Overset grid, Unsteady Euler, Relative motion.

I. Introduction

THE number of algorithms developed for the solution of problems with complex geometries including problems with moving boundaries is substantially increased during the passed ten years. These include algorithms for the solution of flow fields around oscillating airfoils, oscillating objects, moving bodies such as trains passing by each other, store separation, and stage separation, and other problems such as aeroelastic analysis, or flow simulation within internal combustion engines [1-5]. Since the solution domain changes continuously in moving body problems, special care should be paid to retain the quality of grid

Different methods have been developed for the simulation of flow fields with moving boundaries. The simplest approach is to generate a new grid after each time step of solution. Although this approach is desirable for structured grids [6], it cannot be counted as an efficient method, generally. Grid regeneration is a time consuming process, and is questionable in terms of solution accuracy since a great deal of interpolation is required.

S. M. H. Karimian is with the Aerospace Engineering Department, Amirkabir University of Technology, Tehran, Iran (e-mail: hkarim@aut.ac.ir).

, F. S. Salehi, was with the Aerospace Engineering Department, Amirkabir University of Technology, Tehran, Iran. (corresponding author to provide phone: +982164543206; fax: +982166959020; e-mail: fatemehsalehi62@ yahoo.com).

H. Alisadeghi is with the Aerospace Engineering Department, Amirkabir University of Technology, Tehran, Iran. (e-mail: alisadeghi@cic.aut.ac.ir).

The idea of local restructuring was proposed to prevent grid regeneration [7]. In this method the grid is restructured (and not regenerated) merely in regions close to the moving boundaries. However, after several time steps small grid elements will be formed in these regions which should be eliminated. To delay the costly process of element elimination, some researchers perform a smoothening process, such as the one used in dynamic mesh approach of Ref. 8. In this approach nodes are connected to each other with springs. After each step of boundary motion, a uniform grid is formed through the balance of spring forces. Different references have discussed spring factor, K, which is an important parameter in this approach [7, 9]. For the application of dynamic mesh also see Ref. 10. Note that for large motions by which the integrity of grid is destroyed, local re-meshing (or regeneration) still will be required [11].

Some researchers have tried to continuously maintain the quality of grid around the moving bodies. For this purpose the high-quality grid around the body will move with it and will not change during the body motion. In fact, it is the grid far from the body that will be affected by the body motion [12].

The method of overset-grid (Chimera) was initially proposed by Steger et al. [13] and Benek et al [14] to provide a powerful mean of handling the motion of complex geometries on structured grids. The overset-grid method was successfully applied to solve both steady and unsteady Navier-Stokes equations for complex geometries [15-20]. In overset-grid method each body has its own grid. Therefore on each grid, chimera holes are defined in regions where the grid overlaps solid bodies belonging to the other grids. Advantage of chimera grid is its capability to simulate several moving bodies while maintaining a high quality grid around each of them. The disadvantage of chimera grid however, is the large number of interpolations normally required in this method.

Hybrid grids have been used in moving boundary problems [21-25]. In hybrid grid method of Ref. 22, solution domain is divided into three zones. As it will be explained in the next section, general motion of a single body can be simulated easily with these three zones. In this method, the number of node deletion/insertion process and nodal interpolations are minimized to almost nothing. Even in the case of large translational displacements where a node deletion/insertion process is normally required, only a few elements merge together or split.

The objective of this paper is to extend the algorithm of Ref. 22 to the solution of flow field around two bodies in

general motion with respect to each other.

II. Grid Generation Approach

The method of Chimera grid is a grid embedding technique which provides a simple method for the simulation of flow around moving bodies. In this method a background grid is generated around the main body. Around the other bodies independent grids are generated, called minor grids. These minor grids are then overset on the background grid. Between each minor grid and the background grid an overlapping layer is defined to provide means of transferring solution between grids using an interpolation stencil [14, 26, and 27]. When the flow field is being solved on the background grid the region inside the minor grid which is embedded by the overlapping layer is considered as a chimera hole. The region within this hole will not be a part of background solution. In short, Chimera method includes two major components, 1) generation of grids and determination of their overlapping layers, and 2) definition of interpolation functions.

In the present study the method of Ref. 22 which is based on the concept of Chimera grid, is applied for the solution of the flow field around two bodies moving with respect to each other. As shown in Fig. 1. background Cartesian grid is generated within the solution domain. Around the body A, two zones of grids are generated in addition to the background grid. First zone contains the moving body and the surrounding grid, which is fixed to the body and moves with it, and the second zone which has a squared boundary, includes the grid surrounding the first zone. For translational motion of body A first and second zones will move with the body. For rotational motion, however, only the first zone will rotate with the body A. Therefore the general motion of the body A will be simulated with the least node deletion/insertion and interpolation. In the following discussion, the background grid and the two surrounding grids are called grid A.

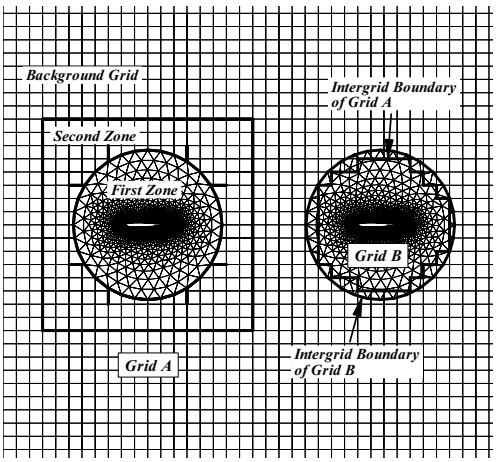

Fig. 1 Grid configuration surrounding body A and B

As about the body B, which will have only rotational motion, any type of grid (structured, unstructured or hybrid grid) can be generated around it. As shown in Fig. 1, a triangular unstructured gird is generated within a circular boundary in the present work; this grid is called grid B. This grid is overset on the background grid. In the present work, solution strategy is to solve the flow field on two sets of grids A and B, separately. When the flow is solved on grid A, the region within the intergrid boundary of grid A is excluded from the solution domain. In this case the boundary values on the intergrid boundary of grid A are interpolated from the solution previously calculated on grid B. On the other hand, when the flow is solved on grid B, the boundary values on the intergrid boundary of grid B are interpolated from the solution previously calculated on grid A. To determine intergrid boundaries, the following procedure is conducted at each step.

On grid A:

1) All of the nodes of grid A, which have a donor cell, are identified. A donor cell is a cell of grid B within which a node of grid A lies.
2) If the distance of these nodes from body A, is less than the average distance of their donor cell vertices from body B, these nodes will be tagged as active nodes for grid A [17].
3) Those cells which all of their vertices are active, are considered active cells. Whereas those cells which none of their vertices are active, will be considered non-active cells. The remaining cells of grid A will be called intergrid-boundary cells.

Similar procedure is applied to Grid B to identify intergrid boundary of grid B.

To clarify the above procedure, consider Fig. 2. Solid and dashed lines denote grid A and grid B, respectively. The donor cell of node *I* which belongs to grid A is indicated by *abc*. If d_I, the shortest distance of this node from body A, is smaller than d_{ave}, the average of shortest distances of node *a*, *b* and *c* from body B, then the node *I* will be an active node. If d_I is larger than d_{ave}, then the node *I* will be a nonactive node.

The overlapping region is shown in Fig. 3. The uppercase and lowercase letters, indicate cells and nodes of grid A. The array IBLANKN is defined for all nodes; its value is 1 for active nodes and 0 for nonactive nods. Similarly, IBLANKC array is defined for all cells as,

$$IBLANKC = \begin{cases} 0 & \text{For nonactive cells} \\ 1 & \text{For active cells} \\ 2 & \text{For intergrid-boundary cells} \end{cases}$$

Therefore the value of these two arrays in Fig.3 would be:

$$\begin{aligned} &IBLANKN(a)=0 \\ &IBLANKN(b)=0 \qquad IBLANKC(A)=0 \\ &IBLANKN(c)=0 \qquad IBLANKC(B)=0 \\ &IBLANKN(d)=0 \;\Rightarrow\; IBLANKC(C)=2 \\ &IBLANKN(e)=1 \qquad IBLANKC(D)=2 \\ &IBLANKN(f)=1 \qquad IBLANKC(E)=1 \\ &IBLANKN(g)=1 \end{aligned}$$

Now, it is clear that based on these values cells *A* and *B* would be nonactive, cell *E* would be active, and cells *C* and *D* would be an intergrid-boundary cell.

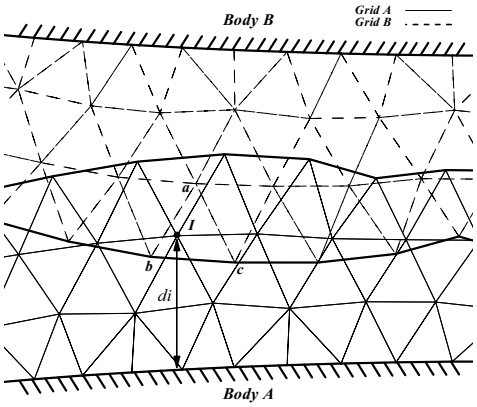

Fig. 2 Determination of intergrid-boundary

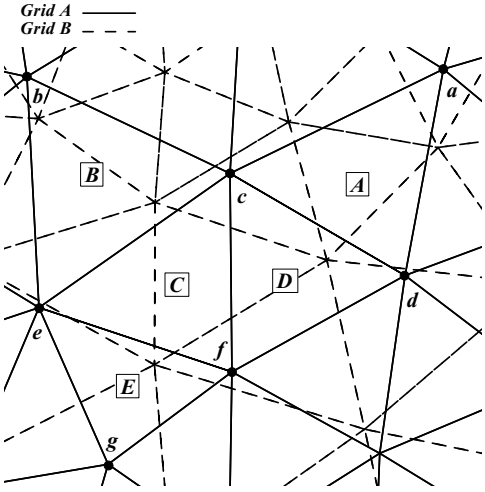

Fig. 3 Determination of active or nonactive nodes and cells

In the present method the two grids are generated independently. This allows us to produce high quality grids. As was mentioned before, body A can have both translational and rotational motions. Due to the grid zones defined around the body A, i.e. a squared zone and a circular zone, both of these motions can be handled very easily with the least node deletion/insertion and interpolation processes. For details about this approach see Ref. 22-24. Body B however, only can have rotational motion. This is not a limitation since the relative translational motion of two bodies is simulated through grid A. Note that all of the elements within the grid B rotate with the body B, and the shape of cells will not change. Figure 4 is presented to clarify this approach of algorithm and the overlapping layers of it. In this figure both airfoils oscillate, however one of them moves in both x and y directions, as well. As seen, depending on the position of airfoils with respect to each other different overlapping grid layers occur. The algorithm is able to correctly determine the overlapping grid layers for complex situation.

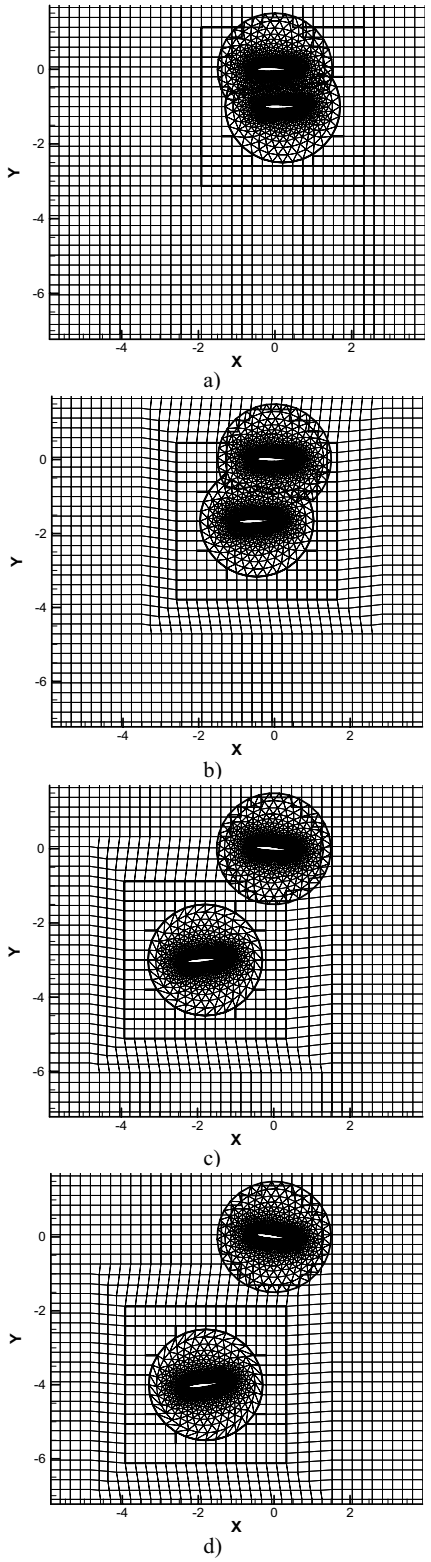

Fig. 4 Some possible grid configurations and their overlapping regions for of two airfoils in motion; a & b) overlapping between two circular grids, c) overlapping out of square region, d) overlapping in square region

If the distance between grid B and second zone of grid A (i.e. the squared boundary region) is not less than a predefined distance, then the rotational or translational motion of body A will not affect the intergrid boundary of grid A. This will obviously lead to ease the solution procedure. Note that this is the case if the body B does not rotate or oscillate by itself. Depending on the number of grid lines on background grid affected by translational motion of body A, the predefined distance can be estimated. While in Ref. 22, always the first grid line of background grid around the second zone is affected by the translational motion of body A, in Ref. 24 it is the first 4 lines that are affected by this motion. This was done by Ref. 24 to effectively prevent the generation of distorted cells.

III. Solution Algorithm

The integral form of two dimensional unsteady Euler equations for compressible flow in the Cartesian coordinate system is given by,

$$\frac{d}{dt}\iint_{\Omega} W dA + \oint_{\partial\Omega}\left(\bar{F}dy - \bar{G}dx\right) = 0 \tag{1}$$

where W, F and G are defined as,

$$W = \begin{pmatrix} \rho \\ \rho u \\ \rho v \\ \rho E \end{pmatrix} \quad \bar{F} = \begin{pmatrix} \rho U \\ \rho u U + p \\ \rho v U \\ (\rho E + p)U + x_t p \end{pmatrix} \quad \bar{G} = \begin{pmatrix} \rho V \\ \rho u V \\ \rho v V + p \\ (\rho E + p)V + y_t p \end{pmatrix} \tag{2}$$

and ρ, p, u, v and E denote density, pressure, velocity components and total energy, respectively. Contravariant velocities U and V are defined as $U=u-x_t$ and $V=v-y_t$

and y_t and x_t are the velocity components of control-volume boundary. In addition to these, equation of state for a perfect gas is used to complete the set of equations. Equation (1) is applied to each of the control volumes with area of Ω and boundary of ∂Ω. This results in the following equation

$$\frac{d}{dt}(w_i\Omega_i) + R_i(w) - D_i(w) = 0 \tag{3}$$

$R_i(w)$ is the convective flux over the surface of control volume i , which is calculated by the Jameson method, and $D_i(w)$ is the numerical dissipative term which is introduced to prevent odd and even point oscillations, and oscillations in the neighborhood of shock waves [28].

A second order accurate Dual Time Stepping scheme is used to calculate unsteady solution. A fully implicit time discretization (in real time) is used to integrate equations (3). In each real time step, then, nonlinear equations are solved using explicit Runge-Kutta multistage scheme or any time-marching method designed to solve steady state problems.

At the far field, non-reflecting boundary conditions are used based on the characteristic analysis. At the solid wall boundary, the normal velocity is set equal to zero, since no mass or other convective fluxes can penetrate the solid body. The pressure value at the solid wall is calculated by extrapolating between its nodal values on the adjacent nodes.

IV. Overset Implementation

As mentioned before Euler equations are solved on two sets of grids with their own intergrid boundaries. The solution procedure at each time step is as follows,

1) On the intergrid boundary edges of grid A, flux values are calculated using flow variables at the neighbor cells. Note that if a cell is nonactive then its flow variable will be interpolated from grid B.
2) Euler equations are solved on grid A, having excluded its nonactive cells from the solution domain.
3) On the intergrid boundary edges of grid B, flux values are calculated using flow variables at the neighbor cells. Note that if a cell is nonactive then its flow variable will be interpolated from grid A.
4) Euler equations are solved on grid B, having excluded its nonactive cells from the solution domain.
5) Again, on the intergrid boundary edges of grid A, flux values are calculated using flow variables at the neighbor cells. An error between these values and those of step 1, called Er_A, is calculated.
6) After exclusion of nonactive cells of Grid A from the solution domain, Euler equations are solved.
7) Again, on the intergrid boundary edges of grid B, flux values are calculated using flow variables at the neighbor cells. An error between these values and those of step 3, called E_{rB}, is calculated.
8) If Er_A and Er_B are less then a defined value, then solution can be preceded to the next time step. Otherwise the above steps should be repeated.

As mentioned above flux values should be calculated on the intergrid boundaries. To clarify the method of this interpolation, consider edge *bc* of grid A, in Fig 5. Figures 5a and 5b show grid configuration before and after removal of nonactive cells of grid A, respectively. To calculate fluxes on this edge, flow variables at cell centers p and q are required. Flow variables at cell center p are obtained from the flow solution on grid A. But, since cell center q belongs to a nonactive cell, flow variables at this cell must be interpolated from their values on grid B; i.e. from their values in donor cell *ijk*. As seen, simple interpolation is used. This means that flow variable on the center of a nonactive cell would be equal to the value of its donor cell.

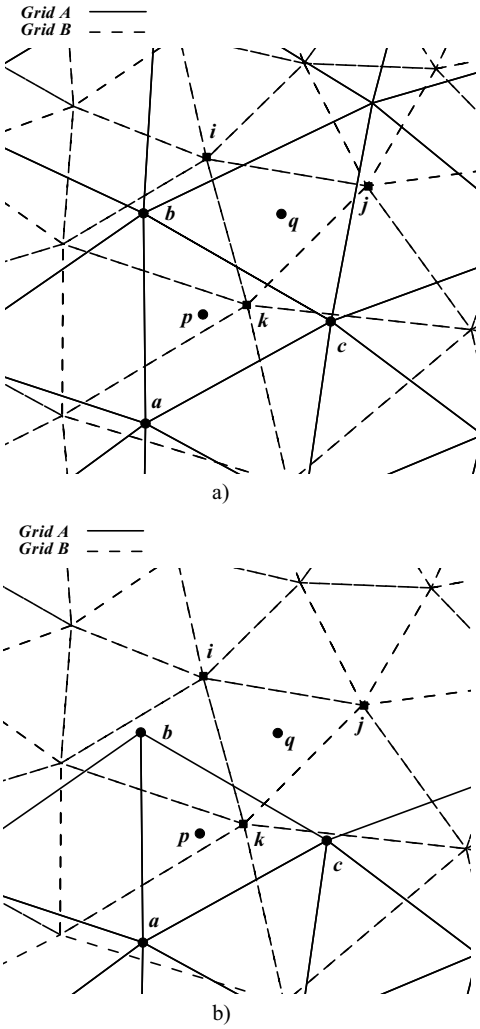

Fig. 5 Overlapping region: a) before and b) after removal of nonactive cells

V. Result and Discussion

In this section the capability of the present method for the simulation of fluid flow over moving bodies are evaluated. The method is validated by comparison of its results with experimental data and numerical results.

First case includes steady state flow of Mach 0.755 at 0.016 degrees angle of attack over a dual airfoil configuration, staggered from each other. The objective of this test is to demonstrate the correctness of solution strategy employed on grids A and B, and the interpolation stencil used in the grid-overlapping region. This is a challenging test case since the strong shock wave between two airfoils crosses the overlapping region. Note that figure 6 shows the overlapping grid layer for the dual NACA0012 airfoils. The existence of shock wave is demonstrated by the pressure contours in Fig. 7. Calculated results clearly show smooth transition of contour lines between two bodies. Figure 8 illustrates the comparison of pressure coefficient distribution on the surfaces of both airfoils with the numerical results of Ref. 20, where Jameson algorithm was used. As seen, present results agree with the results of Ref. 20 excellently.

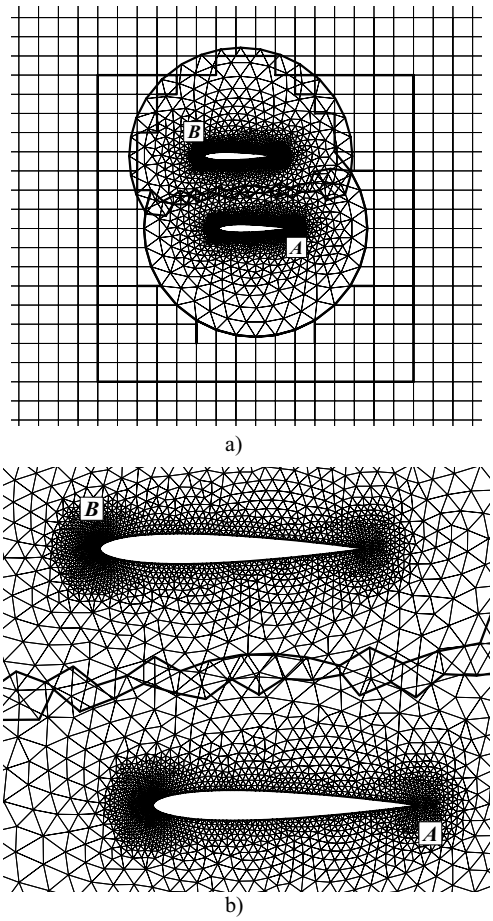

Fig. 6 Grid configuration of 1st case including dual NACA0012 airfoils; a) Overlapping region b) enlarged view of intergrid boundaries

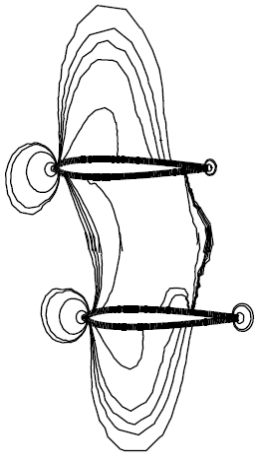

Fig. 7 Pressure contours of flow over dual NACA0012 airfoils; Mach=0.755 and $\alpha = 0.016^{\circ}$

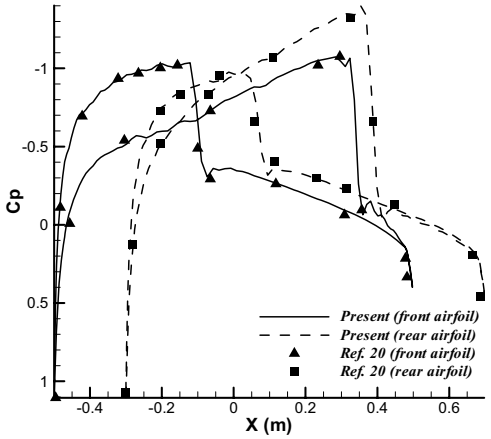

Fig. 8 C_P distribution on the surfaces of the dual NACA0012 airfoils; Mach=0.755 and $\alpha = 0.016^{\circ}$

As the second test case, we would like to solve the unsteady flow over the oscillatory pitching airfoil of NACA 0012, defined in AGARD CT5 test case [29], which has been widely studied in the literature. Consider the harmonic pitching motion of airfoil about the quarter chord of it with the following time dependent varying angle of attack,

$$\alpha = \alpha_m + \alpha_0 \sin \omega t$$

where α_m is the mean angle of attack, α_0 is the amplitude of its oscillation, and ω is the angular frequency of the motion, related to reduced frequency, *k,* by

$$k = \frac{\omega c}{2U_\infty}$$

In this relation, U_∞ is the free stream velocity and *C* is the chord length of the airfoil. Flow conditions are

$$M = 0.755, \quad \alpha_m = 0.016^{\circ}, \quad \alpha_0 = 2.51^{\circ}, \text{and} \quad k = 0.0814$$

In order to demonstrate the correct performance of moving grid algorithm on grids A and B, and the accuracy of interpolation stencil used in the grid overlapping layer for unsteady flow over a rotating body, the above problem is solved on two different grids. As shown in Fig. 9a, flow direction is from left to right and the oscillating airfoil is modeled by grid B; grid A does not contain any body. As about Fig. 9b however, flow is stationary and the oscillating airfoil, modeled by grid A, moves from right to left with the same speed of Mach 0.755. In this case grid B does not contain any body. Therefore, the same flow field is solved on both grids and their results will be compared with each other. Numerical calculation of unsteady flow is started from the steady state solution of Mach 0.755 flow over NACA 0012 airfoil at 0.016 degrees angle of attack on both grids. The variation of normal force coefficient obtained from the present method on both grids is compared with each other and also with the experimental data in Fig. 10. Results obtained on both grids are in excellent agreement with each other. In addition to this, results of the present study agree very well with the results of experiment [29]. The difference between numerical results and experimental data observed here has been reported by other researchers in the literature, as well [10, 22]. This difference can be eliminated if α_m is changed slightly.

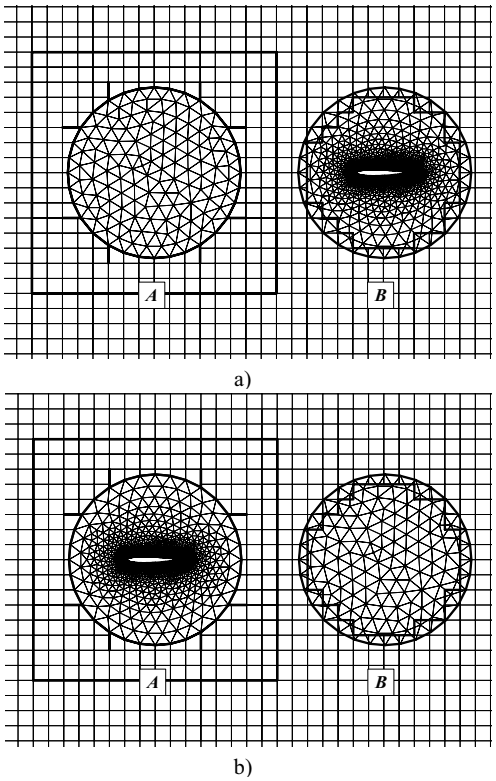

Fig. 9 Illustration of overset grids for 2nd case, i.e. AGARD CT5 case; a) body B and clean grid A, and b) Body A and clean grid B

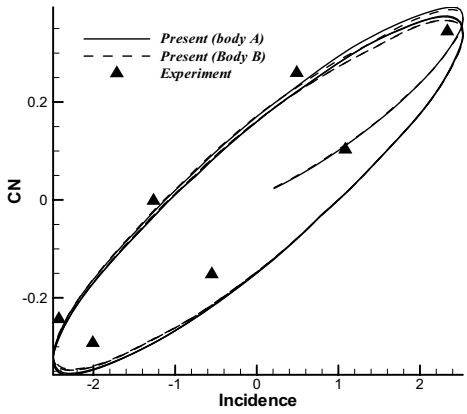

Fig. 10 Comparison of normal-force coefficient loop in 2nd case; including NACA 0012 airfoil at Mach 0.755; present results and experimental data

To validate the algorithm for unsteady flow simulation of translational-rotational motion, the third case is defined here. Again two problems with the same physics of flow field are solved here. As shown in Fig.11, consider two NACA0012 airfoils located at a distance equal to 75 chords from each

other. In the first problem, the left airfoil is stationary and the oscillating airfoil at the right moves toward the left with the speed of Mach 0.5 in a stationary air. In the second problem, the airfoil at the left together with the air move with the speed of Mach 0.5 toward the oscillating airfoil at the right which is stationary. Figure 12 shows the grid structure of this test case when the two airfoils have reached to each other. Parameters governing the oscillating airfoil are

$\alpha_m = 0.016^\circ, \quad \alpha_0 = 2.51, \quad k = 0.0814$

Lift coefficient history of right airfoil obtained from the present method in both problems are compared with each other in Fig. 13. The excellent agreement shows the accuracy of the algorithm for simulation of unsteady problems. Based on the above tests it can be concluded that the present algorithm is well capable of simulating 2-D fluid flow problems with moving bodies.

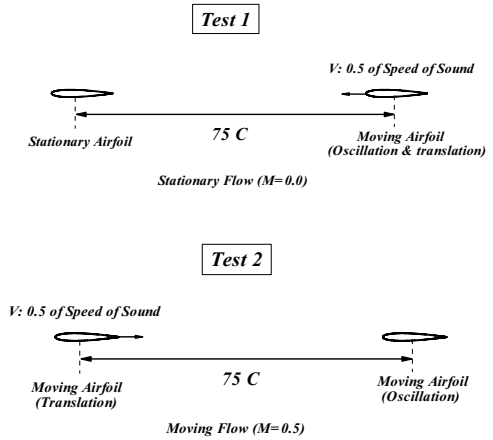

Fig. 11 Illustration of two tests performed for rotational-translational motion of two bodies with respect to each other in 3rd case

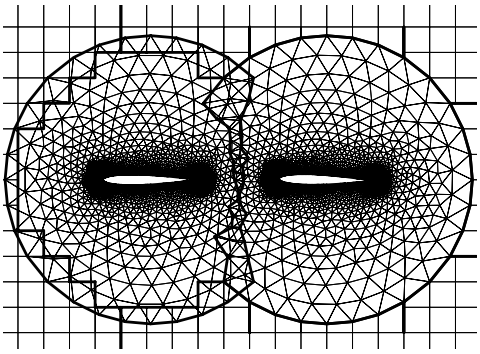

Fig. 12 Grid oversetting at the end of rotational-translational motion of two airfoils when they get close to each other

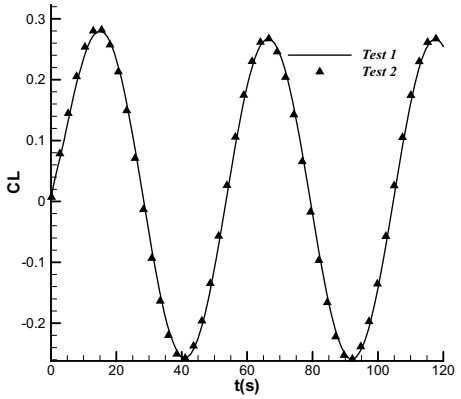

Fig. 13 Lift coefficient history of NACA0012 airfoil for rotational-translational motion, tests 1 and 2 of 3rd case

This forth case is defined to demonstrate the capability of the present method in solving unsteady flows past moving bodies. In this case two oscillating NACA0012 airfoils are positioned in line at a distance of 2.5 chords from each other. Both airfoils are oscillating around their quarter chord in phase. Flow and oscillation conditions are mentioned in second case.

Grid structure around these two airfoils, when zero angle of attack is reached, is illustrated in Fig. 14. Figure 14a and 14b show the coarse and fine grids, respectively. The variation of lift coefficient obtained from the solution of problem on both coarse and fine grids is compared with each other in Fig. 15. Excellent agreement between the results displays accuracy of the present method to simulate unsteady flow around oscillating bodies close to each other. The results show the gird independency

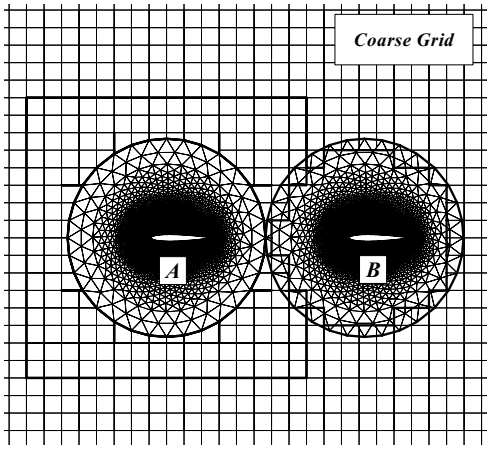

a)

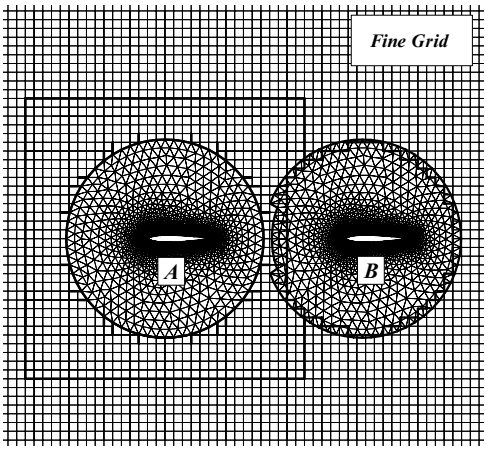

b)

Fig. 14 Grid configuration for two NACA0012 airfoils in 4th case; a) coarse b) fine grids

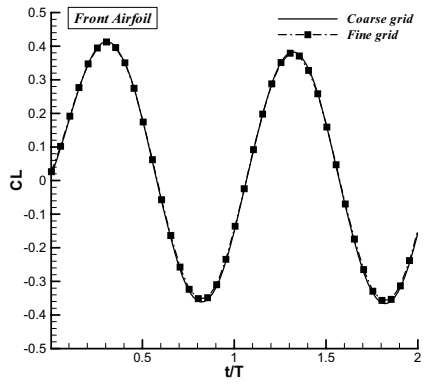

Fig. 15 Instantaneous variation of lift coefficient for two NACA0012 airfoils positioned in line and oscillating in phase

VI. Conclusion

In this paper, a new moving mesh algorithm is developed to simulate the general motion of two bodies with respect to each other. In this method, the overset concept is applied on hybrid grid. This method is based on the algorithm of Ref. 22 which was introduced for the simulation of a rigid body motion. A simple interpolation stencil is used while retaining solution accuracy. The overlapping layer of two grids is determined based on their distances from two bodies. Based on this algorithm, flow field around two bodies in rotation that are in relative translational motion can be simulated. A number of test cases have been solved to prove the capability of present method for accurate solution of flow field around moving bodies. Numerical results agree with experimental data very well. Also to demonstrate correct performance of the present algorithm different benchmark problems have been defined in this paper. In all of the cases present algorithm has resulted in excellent results.

References

[1] J. Sides, K. Pahlke, and M. Costes, "Numerical Simulation of Flows around Helicopters at DLR and ONERA" *Aerosp. Sci. Technol.*, vol. 5, 2001, pp. 35-53.

[2] A. Masud, M. Bhanabhagvanwala, and R. A. Khurram "An Adaptive Mesh Rezoning Scheme for Moving Boundary Flows and Fluid-Structure Interaction" *Computer and Fluids J.*, vol. 36, 2007, pp. 77-91

[3] W. S. Oh, J. S. Kim, O. J. Kwon, "Time-Accurate Navier-Stokes Simulation of Vortex Convection Using An Unstructured Daynamic Mesh Procedure" *Computer and Fluids J.*, vol. 32, 2003, pp. 727-749

[4] C. Farhat, P. Geuzaine, G. Brown, "Application of A Three-Field Nonlinear Fluid-Structure Formulation To The Prediction of The Aerorlastic Parameters of An F-16 Fighter" *Computer and Fluids J.*, vol. 32, 2003, pp. 3-29

[5] Z. Zhang, A. J. Gill, O. Hassan, and K. Morgan, "The Simulation of 3D Unsteady Incompressible Flow with Moving Boundaries On Unstructured Meshes" *Computer and Fluids J.*, vol. 37, 2008, pp. 620-631

[6] A. L. Gationde, "A Dual-Time for Solution of the Unsteady Euler Equation" *Aeronautical J.*, vol. 98, 1994, pp. 283-291

[7] A. Goswami, I. H. Parpia "Grid Restructuring for Moving Boundaries" *AIAA Paper*, No. 91-1589-CP, 1991

[8] Batina, J. T., "Unsteady Euler Algorithm with Unstructured Dynamic Mesh for Complex-Aircraft Aerodynamic Analysis" *AIAA J.*, vol. 29, no. 3, 1991, pp. 327–33.

[9] S. Z. Pirzadeh, "An Adaptive Unstructured Grid Method by Grid Subdivision, Local Remeshing and Grid Movenemt" *AIAA Paper* No. 92-0051, 1992.

[10] A. Jahangirian, and M. Hadidoolabi, "Unstructured Moving Grids for Implicit Calculation of Unsteady Compressible Viscous flow", International Journal for Numerical Methods in Fluids, 2005, 47, pp. 1107-1113.

[11] Y. Zheng, R. W. Lewis, and D. T. Gethin, "Three-Dimensional Unstructured Mesh Generation. Part 1-3" *Computer Methods in Applied Mechanics and Engineering J.,* vol. 134, 1966, , pp. 175-181.

[12] L. P Zhang., Z. J. Wang, "A Block LU-SGS Implicit Dual Time-Stepping Algorithm for Hybrid Dynamic Meshes", *Computers & Fluids J.*, vol. 33, 2004, pp. 891-916.

[13] J. L. Steger, F. C Dougherty., and J. A. Benek, "A Chimera Grid Scheme" in Advances in Grid Generation, American Society of Mechanical Engineers, FED, New York, 1983, Vol. 5, pp. 59-69

[14] J. A. Benek, P. G. Buning, and J. L. Steger, "A 3-D Chimera Grid Embedding Technique" *AIAA Paper* No. 85-1523, 1985

[15] R. L. Meakin, "Moving Body Overset Grid Methods for Complete Aircraft Tiltrotor Simulation" *AIAA Paper* No. 93-3350, 1993.

[16] F. Togashi, K. Nakahashi, Y. Ito, T. Iwamiya, and Y. Shimbo, "Flow Simulation of NAL Experimental Supersonic Airplan/Booster Seperation Using Overset Unstructured Grids*" Computers & Fluids J.,* vol. 30, 2001, pp. 673-688

[17] F. Togashi, Y. Ito, K. Nakahashi, and S. Obayashi, "Extensions of Overset Unstructured Grids to Multiple Bodies in Contact" *J. Aircraft,* vol. 43, no. 1, 2006, pp. 52-57
[18] S. J. Zhang, J. Liu, and Y. S. Chen, "Numerical Simulation of Stage Separation with an Unstructured Chimera Grid Method" *AIAA Paper* No. 2004-4723, 2004.
[19] C. B. Allen, "CHIMERA volume grid generation within the EROS code" Proc. IMechE, Part G: *J. Aerospace Engineering*, 2000, vol. 214, no. 3, pp. 125-141
[20] W. Liao, J. Cai, M. H. Tsai, "A Multigrid Overset Grid Flow Solver with Implicit Hole Cutting Method" *Computer Methods in Applied Mechanics and Engineering J.*, vol. 196, 2007, pp. 1701-1715.
[21] M. J. Aftosmis, M. J. Berger, and J. E. Melton, "Robust and Efficient Cartesian Mesh Generation for Component-Based Geometry" *AIAA Paper* No. 97-0196, 1997
[22] S. M. Mirsajedi, S. M. H. Karimian, and M. Mani, "A Multizone Moving Mesh Algorithm for Simulation of Flow Around a Rigid Body With Arbitrary Motion" *ASME Journal of Fluids Engineering*, vol. 128 2006, pp. 297-304
[23] S. M. Mirsajedi, and S. M. H. Karimian, "Evaluation of A Two-Dimentional Moving-Mesh Method for Rigid Body Mptions" *Aeronautical J.*, vol. , 110, no. 1109, 2006, pp. 429-438
[24] H. Alisadeghi, S. M. H. Karimian, A. R. Jahangirian, "An Implicit Dual Time Stepping Algorithm for Hybrid Dynamic Meshes" in *Proc. 14th Annual Conference of The Computational Fluid Dynamics*, Canada. July 2006
[25] S. Murman, M. Aftosmis, and M. Berger, "Implicit Approaches for Moving Boundaries in A 3-D Cartesian Method" *AIAA Paper* No. 2003-1119, 2003
[26] C. W., Mastin, and H. V. McConnaughey, "Computational Problems on Composite Grids" *AIAA Paper* No. 84-1611, 1984
[27] H. S. Tang, "Study On A Grid Interface Algorithm for Solutions of Incompressible Navier-Stoks Equation" *Computers and Fluids J.*, vol. 35, 2006, pp 1372-1383
[28] A. Jameson, W. Schmidt, and E. Turkel, "Numerical Solution of The Euler Equations by Finite Volume Methods Using Runge-Kutta Time Stepping Schemes" *AIAA Paper* No. 81-1259, 1981
[29] Compendium of Unsteady Aerodynamic Measurements, Report No. AGARD-702, 1982